Modification of source contribution in PALS by simulation using Geant4 code

Xia Ning[1, 2], Xingzhong Cao[2, *], Chong Li[2], Demin Li[1, †], Peng Zhang[2], Yihao Gong[2], Rui Xia[2], Baoyi Wang[2], Long Wei[2]

[1] *Department of Physics, Zhengzhou University, Zhengzhou, 450001, China*

[2] *Beijing Engineering Research Center of Radiographic Techniques and Equipment, Institute of High Energy Physics, CAS, Beijing, 100049, China*

Abstract

The contribution of positron source for the results of a positron annihilation lifetime spectrum (PALS) is simulated using Geant4 code. The geometrical structure of PALS measurement system is a sandwich structure: the ^{22}Na radiation source is encapsulated by Kapton films, and the specimens are attached on the outside of the films. The probabilities of a positron being annihilated in the films, annihilated in the targets, and the effect of positrons reflected back from the specimen surface, are simulated. The probability of a positron annihilated in the film is related to the species of targets and the source film thickness. The simulation result is in reasonable agreement with the available experimental data. Thus, modification of the source contribution calculated by Geant4 is viable, and it beneficial for the analysis of the results of PALS.

Keywords: Positron annihilation lifetime spectrum; Geant4 simulation; Kapton film; Diffusion and reflection; Source contribution

1. Introduction

* Corresponding author. Tel.: 010-88233393; E-mail: caoxzh@ihep.ac.cn;

† Corresponding author. E-mail: lidm@zzu.edu.cn

Positron annihilation spectroscopy technology has unique scientific advantages in applications involving the microcosmic structure of solid materials and thin films. It is a characteristic method for studying materials, defects as vacancies, dislocations, vacancy clusters in metals/alloys, and microstructures as free volumes in polymers or microvoids in micro/mesoporous materials, which can be expressed in a positron annihilation lifetime spectrum (PALS) [1-3]. In the experiment, a sandwich structure is used as the positron source sealed by two pieces of Kapton (or Mylar) films held symmetrically which is called the source film. The source used in the simulations was a point source of ^{22}Na radioactive isotopes [4,5], which are usually used in positron annihilation lifetime measurements. After the positrons are emitted from the source, most are annihilated in specimens; however, there are some positrons would be annihilated in the films. This is called source contribution.

In the measurement of the positron annihilation lifetime, the radioactive isotopes of ^{22}Na used as the positron source can produce a photon with an energy of 1280 keV. A positron is emitted simultaneously. Two photons with an energy of 511 keV are emitted along with the annihilation of a positron-electron after the positrons strike inner materials [6,7]. In the PALS measurement, a 1280 keV photon and two 511 keV photons are detected as the start signal and the stop signals of the positron lifetime, respectively [8-10].

The PALS can be analyzed with deconvolution using specialized programs such as PASFIT and Program LTv9 (LT9) [11,12].The distribution spectrum of positron annihilation in the specimen can be accumulated using the positron annihilation lifetime spectrometer. The spectrum is then analyzed using a former program code to obtain the positron lifetime component in the specimen, as well as the probability and average lifetime of a positron annihilated in the source film. In addition, the resolution of the positron annihilation lifetime spectrometer will be initially settled in the program. Then we can obtain the positron annihilation short-lifetime component τ_1, the intermediate-lifetime component τ_2, the longest-lifetime component τ_3 and the corresponding intensities I_1, I_2 and I_3. The first short-lifetime component τ_1 is attributed to free annihilations of positrons and self-annihilations of p-Ps in the specimen. The intermediate-lifetime component τ_2 is deemed to represent the annihilation of trapped positrons at the defects that are present in the crystalline regions or the annihilations of trapped positrons at the crystalline-amorphous interface

regions. The longest-lifetime τ_3 is attributed to the pick-off annihilations of the ortho-positronium (o-Ps) in the free volume sites present mainly in the amorphous regions of the polymer matrix [13,14]. I_1, I_2 and I_3 are the probabilities of positrons annihilated in the specimen. However, for experiments using positron radiation source, the source contribution should be deducted, thus reducing the impact on measurement results. Therefore, during this procedure, the probability of a positron annihilated in the source film will be settled in the program. We default the lifetime of a source component in the PALS is usually 382 ps with nearly 15% intensity, which can be estimated by measuring the standard specimen, an annealed nickel or iron thin disk [15]. The probability of positron annihilated in the source film used in PALS analysis will affect the results of the lifetime and intensity for the deconvolution. However, some researchers calculate the source contribution, leading to errors in measurement, and many results will deviate to a certain extent. If the contribution of positrons annihilated in the source film is settled appropriately, the positron annihilation lifetime distribution in the specimen can be used to discuss the annihilation mechanism and the microstructures as defects and free volumes in the material. On the contrary, if the probability of a positron annihilated in the source film is inappropriate, the result of the PALS will cause misleading or inaccurate analysis, especially for metal/alloy specimens whose lifetime component for a vacancy cluster is close to 350 ps, and for polymers/porous materials whose lifetime component for a small free volume/microvoid is close to 400 ps [13,16- 22].

An accurate probability of the source film contribution used in the process of analysis of the PALS will contribute to lifetime and intensity results that are more accurate and a better understanding of the positron annihilation mechanism and the material microstructures. In the experiments, the source contribution was usually obtained through the lifetime spectrum deconvolution results of standard specimens. Apart from using the experimental method to estimate the source contribution, it can also be accurately calculated theoretically. In this research, Geant4 code is used to simulate the positrons annihilated in the source film for different specimens that have a layered stacked geometry either symmetrical or non-symmetrical. In this work, the source contributions of mono-energy positrons and real radioactive isotope sources are simulated using Geant4 code, and the discrepancies of source contributions for different specimens are simulated.

When the positrons penetrate a source film, some of the positrons would backscatter, diffuse, or re-emit with a negative work function at the interfaces between the specimen and the film, and subsequently they enter the source film and annihilate. However, the remaining positrons would enter the specimen, and they attain thermal energies in a short period. They will then spread inside the material until eventual annihilation with electrons. In addition, the interactions between positrons and materials are related to the atomic distribution of materials, defects, impurities, and positron energy. Furthermore, external conditions can also affect the interaction between positrons and various basic units in the material. In the present study, the simulation results of source contributions using Geant4 code are reported. The primary positron energies and the incident angles are settled in the range of 1–200 keV and 0–360 degrees, respectively. The positron source is a ^{22}Na radionuclide, and the source films are Kapton, Mylar, and Ni films. The annihilation ratio is simulated by Geant4 code. Finally, we simulate the source contributions of some common materials.

2. Theories and models

Simulations have been used in high energy physics, particle physics and accelerator laboratory experiments. They pose enormous challenges in the creation of complex yet robust software frameworks and applications. With the ever-increasing demand for detector simulations, a professional object-oriented simulation toolkit, Geant4 [23], has been developed. Geant4 is a general toolkit of Monte Carlo simulations for simulating the passage of particles through matter. It has been created using software engineering and object-oriented technology, and it is implemented in the C++ programming language. The toolkit offers a diverse, wide-ranging, but cohesive set of software components that can be employed in a variety of settings. All aspects of the simulation process are included: geometry, materials, fundamental particles, the tracking of particles through materials, as well as comprehensive physics processes, visualization of the detector, and the capture of simulation data. The core of this software system is an abundant set of physics models for handling the interactions of particles with matter across a very wide range of energy. At present, Geant4 is widely used in particle physics, nuclear physics, accelerator design, space engineering, and medical physics.

A PALS with time delays between detecting the 511 keV annihilate photons and the 1280 keV unclear photons is hereafter called the delayed-coincidence spectrum. By analyzing the information of PALS about the positron lifetime τ_i, the corresponding intensities I_i of various groups i of positrons annihilating in a given material can be obtained [24]. The PALS contains a lot of information, therefore some information about the material can be found in order to our need.

The positron lifetime spectrum and Doppler broadening measurement are very important characterization methods, and these characterization methods are very meaningful to the study of the materials. Fig. 1 shows the model structure, which is a sandwich model. The model is symmetrical and the positron source is sealed by the film, and the specimens are attached on the outside of the film. The positrons pass through the film and hit the specimens. During this period, some low-energy positrons will annihilate in the film, however high-energy positrons will enter the specimens until they annihilate with electrons.

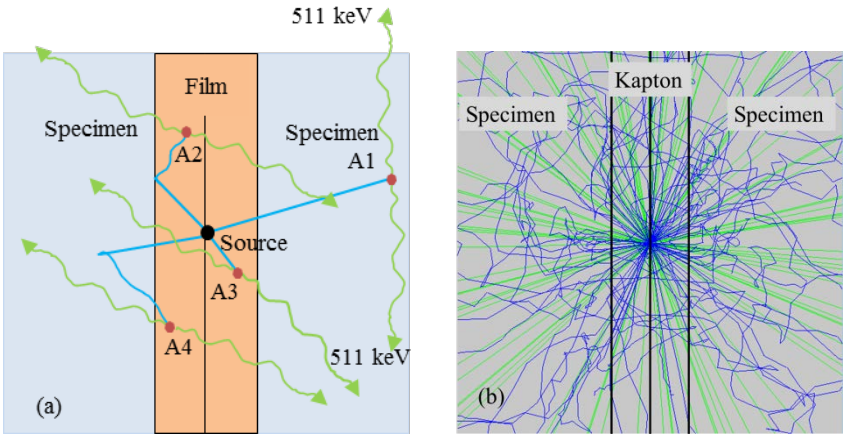

Fig. 1. (a): The side elevation of the model constructed for the simulation, and the demonstration of four positron tracks. A1 shows that the positrons penetrate the film and annihilate in the specimen. A2 shows that the positrons reflect from the interface and annihilate in the film. A3 shows that the positrons annihilate in the film before they enter into the specimen. A4 shows that the positrons enter into the specimen and diffuse back to the film, and then annihilate in the film. The green curve shows the annihilation photons. (b): The trajectory of the positrons emitted from the positron source ^{22}Na radioisotope. Kapton encapsulates the ^{22}Na. The blue line shows the trajectory of a positron and the green line shows the nuclear photons.

The simulation of PALS described here is based on Geant4 and the Origin toolkit. The simulated setup includes a point positron source sealed by two pieces of metal or plastic films (such as Ti, Ni, Kapton, and Mylar films). This is a device with a positron source. In the experiment, to increase the mechanical strength of the source, it was combined with a metal frame around the perimeter of the source; however, it is unnecessary to do so in the Geant4 simulation. In the simulation, the source is placed in between two films.

Typically, for every arrangement of the simulation setup, hundred thousands of source decays are generated. For radionuclide ^{22}Na, a nuclear photon and a positron are generated for every decay, and the positron is generated at a fixed time *t* after the generation of the nuclear photon. The time *t* is very short; therefore, the nuclear photon can be regarded as the start signal. After that, two photons are emitted as a signal of the positron annihilation; therefore, the annihilation photons can be considered as the stop signal.

3. Results and discussion

3.1 Positron distribution in Kapton film

In Geant4 simulation, the emitter is the positron source, which is enveloped by two 7-μm Kapton films, and on both sides of the emitter, 2-mm Al plates were placed. The resulting structure is Al (2 mm)-Kapton-positron source-Kapton-Al (2 mm), which is shown in the inset of Fig. 1. The number of positrons is 2×10^6, and the launch angle is 360 degrees. Moreover, an incident positron is mono-energetic. The energy of a positron ranges from 1–200 keV and the thickness of Kapton ranges from 1–9 μm. After that, we can get the number of positrons annihilating in the Kapton and Al using Geant4 code, for various positron energies and Kapton thicknesses. From Fig. 2, we can get some information about the positrons annihilating in Kapton and Al, thus we can choose a suitable thickness of Kapton and a suitable radionuclide according to the demands of the experiment, and this is very convenient.

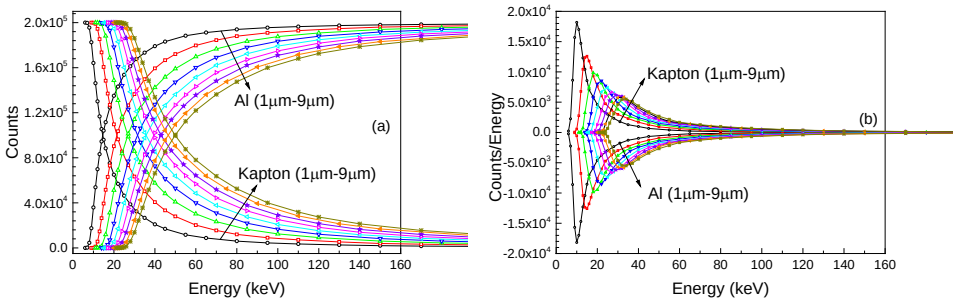

Fig. 2. (a): Number of positrons annihilated in the Kapton and Al with respect to the change of positron energy and Kapton thickness. The increasing curve shows the number of positrons annihilating in Kapton. The decreasing curve shows the number of positrons annihilating in Al. The arrow shows the thickness of Kapton, which is 1 μm to 9 μm; (b): Based on the conclusion from (a), a derivative curve is plotted to show the rate of change of the number of positron annihilations in Kapton and Al.

In Fig. 2, the number of positrons that annihilate in Kapton and Al are simulated using Geant4 code; however, a positron is mono-energetic. If the radioisotope is the positron source, the energy of positrons produced by the radioisotope has a continuous spectrum. In order to make the ^{22}Na radioisotope the positron source, we simulated the energy spectrum of positrons produced from the ^{22}Na radioisotope using Geant4 code. The energy spectrum simulated for the ^{22}Na radioisotope is shown in Fig. 3. In Fig. 3, the full blue line shows the mean kinetic energies of the positrons that are emitted from the ^{22}Na radioisotope. The dashed red line and short dashed purple line show the mean kinetic energies and maximum kinetic energies in the reference [7], respectively.

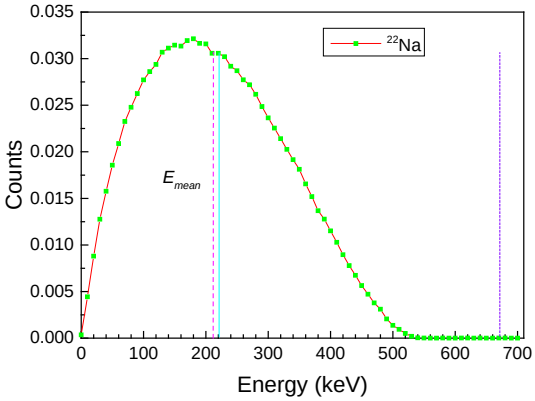

Fig. 3. Simulation of the energy spectrum of the ^{22}Na radioisotope using Geant4 code.

3.2 The radioactive isotope as positron source

In the experiment, the positron source is sealed with a Kapton, Mylar, or metal film when the positron lifetime is being measured. It is known that positrons not only annihilate in a specimen, but also annihilate in a film. Therefore, we should deduct the probability of a positron annihilating in the film when we analyze the PALS. Considering these facts, we simulated the probability of a positron annihilating in the film without specimens using Geant4. As shown in Fig. 4, the source was treated with Kapton, Mylar, Ni, and Ti films using a point positron source ^{22}Na radioisotope in the middle of the film. By changing the thickness of the films, we can obtain the probability of a positron annihilated in the film. In Fig. 4, we find that the probabilities of a positron annihilated in Kapton and Mylar are similar, but it is known that Kapton is resistant to high temperature while Mylar is resistant to both high and low temperatures; therefore, we need to choose the film according to the temperature requirement of the experiment. In Fig. 4, the black vertical line shows the probability of a positron annihilating in the film when the thickness of films is 7 μm [25]. It can be seen that the positron annihilation ratios in the Ni and Ti films are higher than those in the Kapton and Mylar films. Hence, if the positron source is sealed by Ni and Ti films when it is used to measure the positron lifetime, the thickness of the Ni and Ti film should be thinner in order to lose fewer positrons.

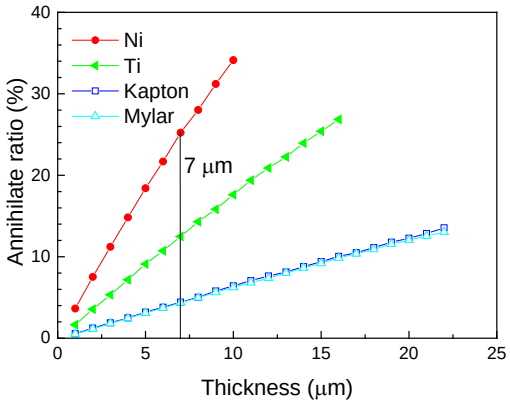

Fig. 4. Simulation of the probability of a positron annihilating in the film without the specimen, the black vertical line shows the probability of a positron annihilating in the film when the thickness of films is 7 μm.

In the presence of the specimens, the positrons that penetrate the film will enter the surface of the specimen; however, some positrons will scatter and return to the positron device. They are treated as new positron sources being localized at the interfaces between the specimen and the film, therefore the probability of a positron annihilating in the film is higher than that without specimens. As shown in Fig. 5, we use ^{22}Na as the positron source, which is sealed by Kapton or Mylar. In addition, metals (Al, Ag, Ni, and Fe) and polymers (High Density Polyethylene (HDPE), Polytetrafluoroethylene (PTFE)) are used as the targets. The thicknesses of the films range from 1–22 μm and the films are semi-infinite targets. Thus, the probability of a positron annihilating in the film for various film thicknesses can be obtained. It is known that the backscattering coefficients vary with different specimens [26-29], therefore the probabilities of a positron annihilating in the film are dissimilar when the specimen is changed. In Fig. 5, it can be seen that, the probability of a positron annihilating in the film is high if the density of the specimen is high.

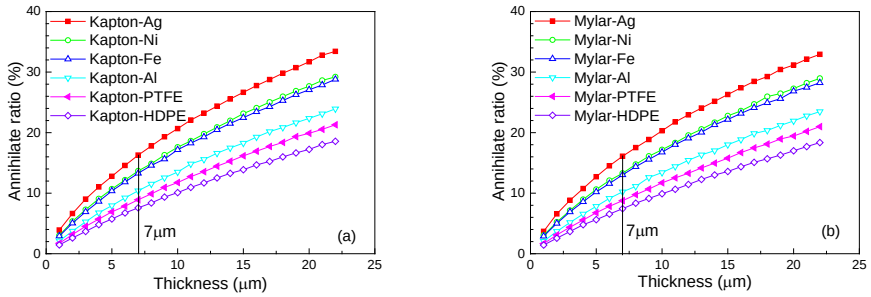

Fig. 5. Simulation of the probability of positron annihilation in the Kapton and Mylar film with changing thickness of the films. (a): Kapton encapsulates the ^{22}Na radioisotope. (b): Mylar encapsulates the ^{22}Na radioisotope. The black line presents the probability of positron annihilation in the film when the thickness of film is 7 μm.

The source is treated as two pieces of 7-μm Kapton film with a point positron ^{22}Na in the simulation [25]. The surrounding stack of films is symmetrical. We performed simulations using Geant4 code, and the results of simulating the implantation profile are shown in Fig. 6. The solid line is based on the bottom-X and left-Y axes, and the dotted line is based on the top-X and right-Y axes.

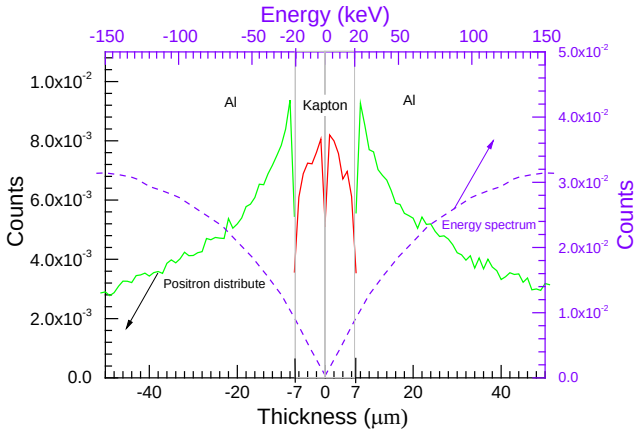

Fig. 6. The solid line shows the implantation profiles for ^{22}Na positrons emitted in the films and Al around the source. The dotted line presents the energy spectrum for the ^{22}Na radioisotope. From Fig. 2 (a), it can be seen that the positrons with an energy less than 20 keV will annihilate in Kapton and the positrons with an energy more than 20 keV will annihilate in Al.

If the positron source is sealed by the metal film, the results will be different from those of the polymer film. As shown in Fig. 7, the thickness of Ni film ranges from 1–10 μm and the specimens are semi-infinite [25]. After that, the probability of positron annihilation in the film for various film thicknesses can be obtained.

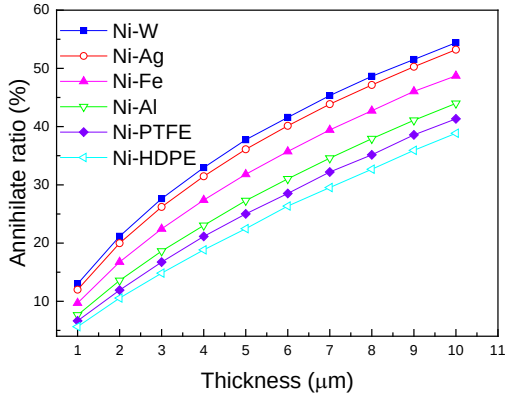

Fig. 7. The probability of positron annihilate in the film with increasing the film thickness when the radioisotope ^{22}Na positron source sealed by Ni film.

In Fig. 5 and Fig. 7, we observe that the probability of a positron annihilating in the film is not only related to the film, but also related to the test specimen. When the positrons hit the specimen, some of the positrons go through the film and enter into the specimen, while others

annihilate in the film, and some positrons will backscatter and enter the film. If the specimen is different and the backscattering coefficient is different, then the probability of a positron annihilating in the film will be different.

The source is treated as two pieces of 7-μm Kapton film with a point positron source ^{22}Na radioisotope between the two films. We simulate the probability of positron annihilation in the film (source contribution) for some common metals, alloys, semiconductors, metal-oxides and polymers, which is shown in Table 1. In Table 1, the arrangement rule of metals is based on the atomic number of the metal. Generally, the source contribution is gradually increased with an increase in the atomic number; however, W is an exception. The metals Ni, W, and Cu are anti-electron modulators and have a negative work function; however, Ni and Cu have an inconspicuous moderated efficiency and the positrons that escape from the metal are very few. Therefore, there is little impact on the source contribution. The moderated efficiency of W is obvious; therefore, more positrons escape from the metal, which influences the source contribution greatly. Therefore, W is special. The arrangement rule of alloys is based on the density of the metal, and the source contribution is gradually increased with increase in density under normal circumstances. The arrangement rule of semiconductors is based on the density, and the source contribution is gradually increased with the increase in density; however, simple substances like Si and Ge do not follow this rule. The arrangement rule of metal-oxides is based on the atomic number of the metal, and the source contribution is gradually increased with an increase in the atomic number. The arrangement rule of polymers is based on the density of the polymer, however the polymer is very special, and the source contribution is not regular. Since the polymer element is very complex, and the source contribution is related to the element, in addition to the density of the polymer.

Table 1: Simulation the source contribution of some common metals, alloys, semiconductors, metal-oxides, and polymers.

Metal	Al	Ti	Cr	Mn	Fe	Co	Ni	Cu	Zn	Ag	W	Pt	Au	Pb
Contr.(%)	10.42	12.42	12.79	13.25	13.29	13.37	13.67	13.72	14.13	16.29	17.63	17.52	17.44	17.58

Alloy	Ti3Al	Fe4C3Si	Fe2C	Fe9Cr	Fe0.6Cu	Fe17Cr14.5Ni	Cu18Zn18Ni	Cu19Ni	Ag5Al
Contr.(%)	12.15	12.98	13.18	13.35	13.29	13.3	13.82	13.82	16.19

Semi	Si	Ge	SiO2	SiC	AlN	Si3N4	ZnS	ZnO	GaN
Contr.(%)	10.61	14.41	9.69	9.79	9.73	9.73	13.04	13.04	13.10
Metal-oxide	MgO	Al2O3	CaO	TiO2	Fe3O4	FeO	CuO	Ag2O	BaO
Contr.(%)	9.63	9.64	10.99	11.04	12.1	12.21	12.99	15.98	16.44
Polymer	HDPE	PEEK	Mylar	PES	PVDF	PCTFE	PVF	PTFE	
Contr.(%)	7.57	8.06	8.31	8.6	10.53	9.64	8.27	8.91	

4. Modification of the PALS of Ni, Fe, HDPE, and PTFE

The acquired lifetime spectra were resolved into two-lifetime components in some crystal and defect-free specimens such as metals/alloys and semiconductors, or three-lifetime components in some specimens with defects and polymers with free volumes, and to lesser extent four-lifetime components in some porous materials with micro/mesoporous properties and voids or some polymers with open free volume space.

Generally, the default source contribution would be the same if either polymers or metals are used as specimens for analyzing the PALS. However, from the simulated data using Geant4, we observe that the source contribution is different for different specimens. In order to compare the difference between the source contribution using Geant4 simulation and the experimental results when analyzing the positron annihilation lifetime, we measure some specimens, including standard specimens of metals Ni and Fe (note: the metals Ni and Fe were obtained by annealing, so defects may exist) [15], and polymers HDPE and PTFE (as shown in Table 2). Each lifetime measurement lasted for four hours. The specimens are semi-infinite. ^{22}NaCl is used as the positron source and radioactive ^{22}NaCl is sealed using Kapton films when the specimens are being measured. The thickness of the films is 7 μm. In the experiment, the source contribution is obtained by measuring a standard specimen. The PALS of Ni, Fe, HDPE, and PTFE are analyzed with the program LTv9 (see Table 2) [12]. In Table 2, for the cases of standard Ni and Fe, the “Free” (the analyzed spectrum with three components) shows that by fixing the source contribution to 0 and the τ_2 to 382 ps, we can obtain the lifetime τ with the intensity I. The “Fix” (the analyzed spectrum with two components) shows that the source contribution is I_2 and the positron lifetime in the source is 382 ps. For the cases of HDPE and PTFE, the “Free” shows that the source contribution is absent, and the “Fix” shows that the source contribution is 17.74% (Ni). Using Geant4 code, we obtain the probabilities of positron annihilation in the film which are

13.67%, 13.29%, 7.57% and 8.91% for specimens Ni, Fe, HDPE and PTFE, respectively. Under normal conditions, the positron annihilation lifetime in Kapton is shorter than 382 ps; however, the annihilation lifetime of a positron backscattered from the specimen surface to be annihilated in Kapton is longer than 382 ps, therefore the default is 382 ps. Therefore, in the source, the default positron annihilation lifetime is 382 ps in the experiment and the simulation.

In Table 2, the intensity of the positron annihilation longest-lifetime component τ_3 is high, because the positron source has been used for a long time and the positron source residue of NaCl is no longer radioactive; therefore, some low-energy positrons will annihilate in NaCl.

Table 2: Results of PALS for Ni, Fe, HDPE, and PTFE [11,17,18,30-33]. Experiment: the source contribution is obtained by measuring the standard specimen. Simulation: the probability of positron annihilation in the film using Geant4 code; the source contribution is different when the specimens differ.

Specimen		Source Contr.	τ_1 (ps)	I_1 (%)	τ_2 (ps)	I_2 (%)	τ_3 (ps)	I_3 (%)	Source	
									Contr.(%)	Lifetime(ps)
Ni	Exp.	Free	106.0±0.28	80.99±0.06	382.0	17.74±0.06	2579±25	1.27±0.01	--	--
		Fix	106.0±0.12	98.46±0.01	2579±22	1.54±0.01	--	--	17.74	382
	Sim.		117.0±0.14	98.07±0.01	1997±9.6	1.94±0.01	--	--	13.67	382
Fe	Exp.	Free	104.7±0.27	81.52±0.06	382.0	17.32±0.06	2571±26	1.16±0.01	--	--
		Fix	104.7±0.12	98.59±0.01	2571±21	1.41±0.01	--	--	17.32	382
	Sim.		115.6±0.18	98.20±0.01	1954±15	1.80±0.01	--	--	13.29	382
HDPE	Exp.	Free	175.2±3.2	42.85±0.80	447.0±6.1	43.04±0.74	2305±13	14.11±0.23	--	--
		Fix	173.5±2.2	50.49±0.52	483.1±6.6	32.50±0.55	2316±8.1	17.01±0.19	17.74	382
	Sim.		178.0±2	45.75±0.56	467.5±5.9	38.97±0.57	2346±9.1	15.28±0.19	7.57	382
PTFE	Exp.	Free	215.4±2.1	56.29±0.50	590.2±7.3	32.30±0.49	3606±18	11.41±0.13	--	--
		Fix	204.8±1.9	59.40±0.39	668.7±9.3	27.02±0.38	3659±21	13.58±0.14	17.74	382
	Sim.		214.0±2.1	57.52±0.46	632.5±8.2	30.00±0.45	3685±21	12.48±0.14	8.91	382

In actual measurements, we measure the standard specimen to determine the source contribution. However, the actual condition is quite complex, and the source contribution will be different for different specimens, so the source contribution has a certain influence on the analysis of the PALS. In Table 2, τ_1 represents the positron lifetime in the metal for standard specimens Ni and Fe. It shows that τ_1 is the same both with and without source contribution, and only the intensity is different. Nevertheless, the positron lifetime in the polymer is different since the polymer has defects and vacancies. In Table 2, we observe that the short-lifetime component τ_1 is

longer and the lifetime τ_2 is shorter when we compare the simulation result by using Geant4 with the experimental result. However, the corresponding intensity I_1 is decreasing, I_2 is increasing, the longest-lifetime τ_3 is longer, and the corresponding intensity I_3 is decreasing, so we expect that the effect of source contribution is more prominent in the experiment.

5. Conclusions

The positron annihilation ratios in source films (Kapton, Mylar and Ni films) for various film thicknesses were calculated using Geant4 code, and the modification of source contributions for some common materials (metals, alloys, semiconductors, metal-oxides, and polymers) is summarized in this paper. It was found that the source contribution is related to the properties of the specimens (type, thickness, and so on). The annihilation ratio increases with an increase in film thickness, and the value of the annihilation ratio for the Ni film was larger than that for the Kapton and Mylar films. When we used the ^{22}Na radioisotope as the positron source and the source film was 7-μm Kapton, the source contributions were 10%–18%, 10%–14%, 9%–17%, and 7%–11% for metal/alloys, semiconductors, metal-oxides, and polymers, respectively. The source contribution was fixed for some common materials, as reported in previous studies. However, when we compared the source contribution difference between the simulation results of Geant4 and the experimental results for the PALS of Ni, Fe, HDPE, and PTFE, the results simulated using Geant4 were found to be more reasonable. The source contribution was optimized by Geant4 simulation, and these simulated data provided a theoretical basis for the analysis of the positron lifetime spectrum in the experiment.

Acknowledgements

This work was supported in part by the National Natural Science Foundation of China (No. 11475197, 11575205, 11475193).

References

[1] S. Dutta, M. Chakrabarti, S. Chattopadhyay, D. Jana, D. Sanyal, A. Sarkar, Defect dynamics in annealed ZnO by positron annihilation spectroscopy, J. Appl. Phys. 98 (2005) 053513.

[2] A.C. Krusema, H. Schut, A. van Veen, M. Fujinami, Oxygen implanted silicon investigated by

positron annihilation Spectroscopy, Nucl. Instr. Meth. Phys. Res. B 148 (1999) 294-299.

[3] K. Saarinen, P. Seppälä, J. Oila, P. Hautojärvi, C. Corbel, O. Briot, R.L. Aulombard, Gallium vacancies and the growth stoichiometry of GaN studied by positron annihilation spectroscopy, Appl. Phys. Lett. 73 (1998) 3253.

[4] S.K. Sharma, J. Prakash, J. Bahadur, K. Sudarshan, P. Maheshwari, S. Mazumder, P.K. Pujari, Investigation of nanolevel molecular packing and its role in thermo-mechanical properties of PVA–fMWCNT composites: positron annihilation and small angle X-ray scattering studies, Phys. Chem. Chem. Phys. 16 (2014)1399-1408.

[5] D.B. Cassidy, S.H.M. Deng, H.K.M. Tanaka, A.P. Mills, Single shot positron annihilation lifetime spectroscopy, Appl. Phys. Lett. 88 (2006) 194105.

[6] R.A. Dunlap, J. Kyriakidis, Z. Wang, D.W. Lawther, A Doppler broadening positron annihilation technique for the study of defects in bulk samples, Nucl. Instr. Meth. Phys. Res. B 108 (1996) 339-342.

[7] L. Jødal, C.L. Loirec, C. Champion, Positron range in PET imaging: non-conventional isotopes, Phys. Med. Biol. 59 (2014) 7419–7434.

[8] E.A. Badawi, M.A. Abdel-rahman, S.A. Mahmoud, Investigation of defects (migration and formation) in metals by positron annihilation lifetime, Appl. Surf. Sci. 149 (1999) 211–216.

[9] N. Meyendorf, G. Dlubek, A. Surkov, Positron annihilation spectroscopy to study nanoprecipitations in aluminum alloys, SPIE Proc. 5392 (2004) 54-62.

[10] P. Winberg, M. Eldrup, F.H.J. Maurer, Nanoscopic properties of silica filled polydimethylsiloxane by means of positron annihilation lifetime spectroscopy, Polymer 45(24) (2004) 8253–8264.

[11] J. Kansy, Microcomputer program for analysis of positron annihilation lifetime spectra, Nucl. Instr. Meth. Phys. Res. A 374 (1996) 235-244.

[12] C. Pascual-Izarra, A.W. Dong, S.J. Pas, A.J. Hill, B.J. Boyd, C.J. Drummond, Advanced fitting algorithms for analysing positron annihilation lifetime spectra, Nucl. Instr. Meth. Phys. Res. A 603 (2009) 456–466.

[13] R.F. Bhajantri, V. Ravindrachary, A. Harisha, C. Ranganathaiah, G.N. Kumaraswamy, Effect of barium chloride doping on PVA microstructure: positron annihilation study, Appl. Phys. A 87 (2007) 797–805.

[14] W.C. Chao, S.H. Huang, Q.F. An, D. Liaw, Y.C. Huang, K. Lee, J. Lai, Novel interfacially-polymerized polyamide thin-film composite membranes: Studies on characterization, pervaporation, and positron annihilation spectroscopy, Polymer 52 (2011) 2414-2421.

[15] X.Z. Cao, Q. Xu, K. Sato, T. Yoshiie, Effects of dislocations on thermal helium desorption from nickel and iron, J. Nucl. Mater. 417 (2011) 1034-1037.

[16] R. Idczak, R. Konieczny, J. Chojcan, A study of defects in iron-based binary alloys by the Mössbauer and positron annihilation spectroscopies, J. Appl. Phys. 115 (2014) 103513.

[17] H. Li, M. Maekawa, A. Kawasuso, N. Tanimura, Effect of magnetic field on positron lifetimes of Fe, Co and Ni, J. Phys.: Condens. Matter 27 (2015) 246001.

[18] J. Jiang, Y.C. Wu, X.B. Liu, R.S. Wang, Y. Nagai, K. Inoue, Y. Shimizu, T. Toyama, Microstructural evolution of RPV steels under proton and ion irradiation studied by positron annihilation spectroscopy, J. Nucl. Mater. 458 (2015) 326-334.

[19] Z. Kargar, S.M. Asgarian, M. Mozaffari, Positron annihilation and magnetic properties studies of copper substituted nickel ferrite nanoparticles, Nucl. Instr. Meth. Phys. Res. B 375 (2016) 71-78.

[20] P.V. Kuznetsov, Y.P. Mironov, A.I. Tolmachev, T.V. Rakhmatulina, Y.S. Bordulev, R.S. Laptev, A.M. Lider, A.A. Mikhailov, A.V. Korznikov, Positron annihilation spectroscopy of vacancy-type defects hierarchy in submicrocrystalline nickel during annealing, AIP Conf. Proc. 1623 (2014) 327-330.

[21] S.D. Praveena, V. Ravindrachary, R.F. Bhajantri, Ismayil, Dopant-Induced Microstructural, Optical, and Electrical Properties of TiO2/PVA Composite, Polym. Compos. 37(4) (2016) 987–997.

[22] G. Dlubek, K. Saarinen, H.M. Fretwell, Positron states in polyethylene and polytetra-uoroethylene: A positron lifetime and Doppler-broadening study, Nucl. Instr. Meth. Phys. Res. B 142 (1998) 139-155.

[23] S. Agostinelliae, J. Allisonas, K. Amako, J. Apostolakis, H. Araujo, Geant4—a simulation toolkit, Nucl. Instr. Meth. Phys. Res. A 506 (2003) 250-303.

[24] L.Y. Dubov, V.I. Grafutin, Y.V. Funtikov, Y.V. Shtotsky, L.V. Elnikova, Optimization of BaF2 positron-lifetime spectrometer geometry based on the Geant4 simulations, Nucl. Instr. Meth. Phys. Res. B 334 (2014) 81-87.

[25] K. Siemek, J. Dryzek, The Computer Code for Calculations of the Positron Distribution in a Layered Stack Systems, Acta Phys. Pol. A 125(3) (2014) 833-836.

[26] S.J. Huang, Z.W. Pan, J.D. Liu, R.D. Han, B.J. Ye, Simulation of positron backscattering and implantation profiles using Geant4 code, Chin. Phys. B 24 (10) (2015) 107803.

[27] P.G. Coleman, L. Albrecht, K.O. Jensent, A.B. Walker, Positron backscattering from elemental solids, J. Phys.: Condens. Matter (41992) 10311-10322.

[28] J. Mäkinen, S. Palko, J. Martikainen, P. Hautojarvi, Positron backscattering probabilities from solid surfaces at 2-30 keV, J. Phys.: Condens. Matter 4 (1992) L503-L508.

[29] X. Lai, X.P. Jiang, X.Z. Cao, X. Zhang, Z.M. Zhang, X.X. Cao, G. Xiang, B.Y. Wang, L. Wei, Simulation of positron backscattering on Al, Cu, Ag and Au targets using GEANT4 code, Surf. Interface Anal.(2016) DOI: 10.1002/sia.6179.

[30] M. Premila, S. Abhaya, R. Rajaraman, T.R. Ravindran, G. Amarendra, C.S. Sundar, Probing the local structural changes across the amorphous to crystalline transition in iron phosphate glass: Positron annihilation and micro Raman studies, J. Non-Cryst. Solids 358 (2012)

1014-1018.

[31] M. Fukuhara, Vacancy analysis in a Ni-Nb-Zr-H glassy alloy by positron annihilation spectroscopy, Appl. Phys. Lett. 100 (2012) 093102.

[32] S.J. Jia, Z.C. Zhang, Y.M. Fan, H.M. Weng, X.F. Zhang, R.D. Hang, Study of the size and numerical concentration of the free volume of carbon filled HDPE composites by the positron annihilation method, Eur. Polym. J. 38 (2002) 2433-2439.

[33] M.M. Madani, R.C. Macqueen, R.D. Cranata, Positron Annihilation Lifetime Study of PTFE/Silica Composites, J. Polym. Sci., Polym. Phys. B 34 (1996) 2767-2770.